# Pressure-induced shift and broadening of 1510–1540-nm acetylene wavelength calibration lines

**W. C. Swann and S. L. Gilbert**

*Division of Optoelectronics, Electronics and Electrical Engineering Laboratory, National Institute of Standards and Technology, Boulder, Colorado 80303*

Received November 1, 1999; revised manuscript received January 24, 2000

We have measured the pressure-induced shift for 15 lines of the $\nu_1 + \nu_3$ rotational–vibrational band of acetylene $^{12}C_2H_2$. These lines are useful as wavelength references in the 1510–1540-nm region. We find that the pressure shift varies from +0.008(2) pm/kPa for line $R1$ to +0.043(2) pm/kPa for line $R27$, with many of the lines exhibiting a shift near +0.017 pm/kPa (or, equivalently, $+2.3 \times 10^{-3}$ pm/Torr or −0.29 MHz/Torr). In addition, we have measured the pressure broadening of these lines and find that it also varies with line number and is typically ~0.7 pm/kPa (~12 MHz/Torr). We also evaluate the line sensitivity to temperature changes and electromagnetic fields. [S0740-3224(00)01007-9]

*OCIS codes:* 020.3690, 060.2330, 120.3940, 120.4800, 300.6260, 300.6390, 300.0300.

## 1. INTRODUCTION

Wavelength references are important in the 1500-nm region to support wavelength-division-multiplexed optical fiber communication systems. In a wavelength-division-multiplexed system many wavelength channels are sent down the same fiber, thereby increasing the bandwidth of the system by the number of channels. If one channel's wavelength were to shift, cross talk could occur between that channel and a neighboring channel. To calibrate instruments that are used to characterize components and monitor the wavelengths of the channels, wavelength references are needed.

Fundamental atomic or molecular absorptions provide wavelength references that are stable under changing environmental conditions such as temperature and pressure variations or the presence of electromagnetic fields. There are several good molecular transitions in the 1500-nm region. The acetylene $^{12}C_2H_2$ $\nu_1 + \nu_3$ rotational–vibrational combination band, shown in Fig. 1, contains ~50 strong lines between 1510 and 1540 nm. The corresponding band in $^{13}C_2H_2$ extends from ~1520 to ~1550 nm. Hydrogen cyanide also has a good spectrum, with lines between 1530 and 1565 nm for $H^{13}C^{14}N$. The National Institute of Standards and Technology (NIST) has developed wavelength calibration transfer standards based on acetylene and hydrogen cyanide.[1,2]

The vacuum wavelengths of the acetylene $\nu_1 + \nu_3$ lines have been measured at low pressure with an uncertainty of $\sim 10^{-6}$ nm.[3] For a wavelength reference, the stability of the wavelength of each absorption line is a critical characteristic. The symmetric isotopic species of acetylene are particularly insensitive to external perturbation because they have no permanent dipole moment. The largest potential source of line shift is energy-level shift caused by the interaction of the molecules during elastic collisions.[4] Commonly called the pressure shift, this shift depends linearly on the collision frequency. An upper limit for the pressure shift of 200 kHz/Torr (1.5 kHz/Pa) has been reported for one acetylene line at low pressure.[5] For wavelength calibration of instruments, however, it is often desirable to use an intermediate- or high-pressure sample to match the reference bandwidth to the instrument resolution. This results in the strongest signals for a given resolution bandwidth.

We have measured the pressure-induced shift and broadening for 15 lines in the $\nu_1 + \nu_3$ rotational–vibrational band of acetylene $^{12}C_2H_2$. We describe our measurement procedure in Section 2 and summarize the results in Section 3. In Section 4 we estimate the line center sensitivity to temperature changes and electromagnetic fields. Conclusions are given in Section 5.

## 2. MEASUREMENT DESCRIPTION AND DATA ANALYSIS

A schematic diagram of our pressure shift measurement apparatus is shown in Fig. 2. Light from a tunable diode laser is sent through two absorption cells simultaneously, and the transmission through each cell is monitored by detectors. One cell contains acetylene gas at low pressure, and the other contains either intermediate or high pressure, as specified below. A third detector monitors the laser power, and a wavelength meter measures the laser's wavelength with an uncertainty of 1 part in $10^7$ (0.15 pm at 1500 nm). A computer controls the laser wavelength scan and records the readings of the three detectors and wavelength meter.

Three absorption cells were filled with acetylene $^{12}C_2H_2$ at low pressure (6.7 ± 0.1 kPa, ~50 Torr), intermediate pressure (29.7 ± 0.5 kPa, ~225 Torr), and high pressure (66 ± 1 kPa, ~500 Torr). The pressure uncertainty quoted here is the expanded uncertainty obtained with a

0740-3224/00/071263-08$15.00

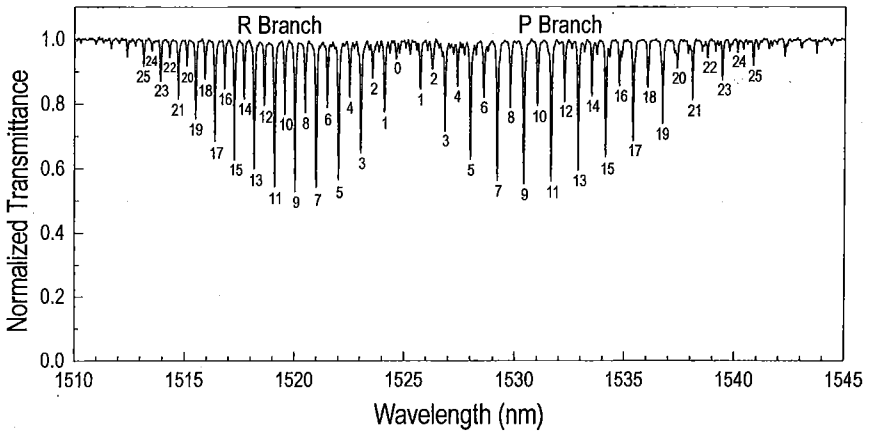


Fig. 1. Acetylene ($^{12}C_2H_2$) spectrum taken by passing LED light through a 5-cm-long absorption cell and recording the spectrum of the transmitted light with an optical spectrum analyzer with 0.05-nm resolution. This spectrum has been normalized to the LED spectrum.

coverage factor $k = 2$ (i.e., our quoted uncertainty is $\pm 2\sigma$).[6] The fused-silica absorption cells are 5 cm long, with windows fused to the cells by a glass frit method. To prevent interference fringes in the transmitted signal the windows are mounted at an angle of 11° and are also wedged by ~2°. The cells were first evacuated and leak checked and were then filled with isotopically pure gas (99.96% $^{12}C_2H_2$). During the fill process the pressure in the fill manifold (and hence the cell) was monitored with a capacitance manometer and a strain gauge pressure sensor. Once filled, the cells were closed off with a glass valve with o-ring seals.

Figure 3 shows spectra of line $P4$ obtained with the low- and the high-pressure cells. The pressure broadening in the high-pressure spectrum is obvious. We are primarily interested in the shift of the high-pressure line relative to the low-pressure line. Fifteen lines were scanned by this technique, and 13 of these lines were also scanned by use of the low- and the intermediate-pressure cells. The measured quantity, the transmitted power $I_T$, is related to the absorption coefficient $\alpha$ and the absorption path length $L$ by

$$I_T = I_0 \exp(-\alpha L), \tag{1}$$

where $I_0$ is the incident power. We first divided the cell transmission curves by the laser power monitor signal to remove common-mode intensity variations and normalized the data. We then took the natural logarithm to obtain the absorbance $\alpha L$.

Individual lines were then fitted to Voigt profiles[4] by use of an orthogonal distance regression algorithm.[7] The orthogonal distance regression, called either error-in-variables or total-least-squares regression, obtains the model parameters by minimizing the sum of squares (SS) of the orthogonal distances from the model to the data points. The fitting program was able to account for a background slope and uncertainties in both $x$ (wavelength) and $y$ (transmitted power). A Voigt profile is a convolution of Lorentzian and Gaussian profiles; it results when there is a combination of Gaussian broadening (resulting from Doppler broadening, for example) and Lorentzian line shape (resulting from the natural linewidth or pressure broadening, for example). In our situation the natural linewidth is small compared with the

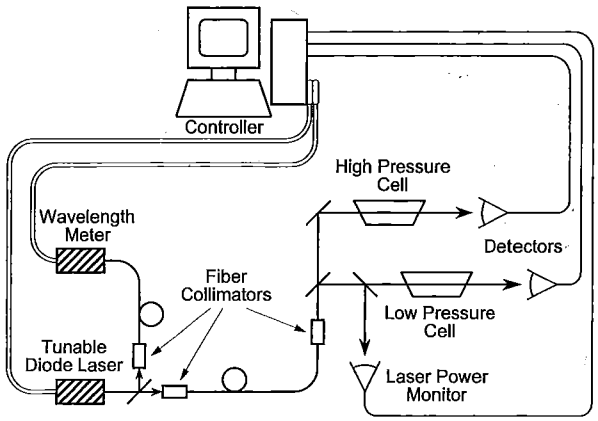


Fig. 2. Diagram of pressure shift measurement apparatus.

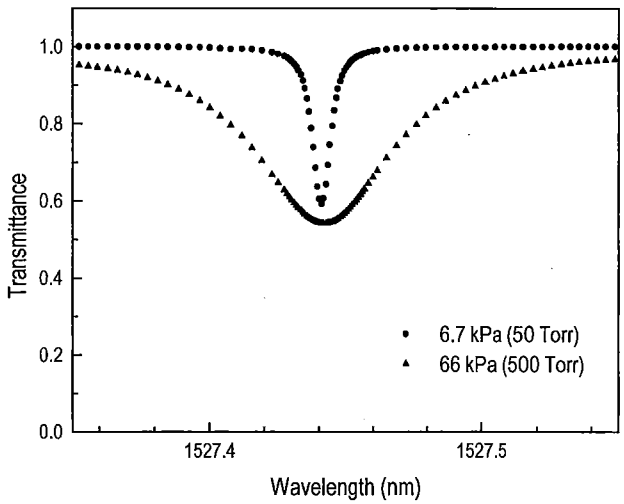


Fig. 3. Tunable diode laser scan of the $^{12}C_2H_2$ line $P4$ showing the transmittance through the low- and the high-pressure cells.

Gaussian Doppler broadening and the Lorentzian pressure broadening. For the low-pressure data, the width of the Lorentzian component and the width of the Gaussian component are comparable. For the intermediate- and the high-pressure data, the Lorentzian component dominates because of the larger pressure broadening. For the

line fitting, we fixed the Gaussian Doppler linewidth at 3.7 pm (Ref. 4) and allowed other model parameters to vary.

Since the spectra for the low- and the high-pressure cells were measured simultaneously, the absolute accuracy of the wavelength meter was not of critical importance for the relative pressure shift measurement. However, the short-term statistical variation of the wavelength measurement did add noise to the data. To determine this statistical variation we took repeated measurements of a laser stabilized to a narrow rubidium line. The statistical variation of repeated measurements yielded a Gaussian distribution with a standard deviation of 0.1 pm. We determined the experimental uncertainty in transmitted power by measuring the statistical variation of the data within a region of the line wing. The standard deviation of these fluctuations was 1 part in $10^4$ of the transmitted power.

Each data point was assigned a standard uncertainty of 0.1 pm for the wavelength and a fractional uncertainty of 1 part in $10^4$ for the transmitted power. The fitting program determined the line centers and their widths, the corresponding uncertainties, and the reduced residual-SS ($\chi^2$) value for the fit. Several factors can complicate the fitting procedure and can cause uncertainty in the line center measurement. Our approaches to minimizing and measuring the effect of these contributions are discussed below.

### A. Background Signal Variation

A slope or a variation in the background level can shift the apparent center of a line, particularly for the wide lines of the intermediate- and the high-pressure cells. Interference fringes due to reflected laser light, wavelength dependence of the optical components, beam pointing stability, and variations in the laser power can cause background variation. As mentioned above, we removed common-mode laser power variations by dividing the cell transmittance data by the power monitor data. Owing to the wavelength dependence of optical fiber couplers (splitters), we used free-space beam splitters to send the laser light to the cells and the power monitor. We minimized interference effects by using wedged cell windows and beam splitters, windowless detectors, and two optical isolators. These measures reduced the statistical power fluctuations to 1 part in $10^4$ and the residual slope to less than 5 parts in $10^4$ over a 250-pm scan. This residual slope was ~1 order of magnitude less than that caused by small spectra features discussed below and is consequently insignificant compared with spectral effects.

### B. Overlap with Nearby Lines

Wings of nearby lines can skew the shape of the line being measured and can shift its apparent center. In addition to the strong lines of the $\nu_1 + \nu_3$ band, there are a number of weak lines throughout the spectrum that are due to hot bands (transitions that are not out of the ground vibrational state).[8] Figure 4 is a plot of the absorbance between 1526 and 1529 nm, showing lines $P2$–$P6$ of the $\nu_1 + \nu_3$ band and weaker hot band lines. To minimize the effect of neighboring lines on our pressure shift measurement we deliberately avoided measuring lines in the spectrum that have significant lines very close to the primary line (such as line $P2$). We used high-resolution spectra[8] to select lines that were relatively isolated from other lines. This eliminated the large perturbations, but some smaller lines were present in the vicinity of several measured primary lines.

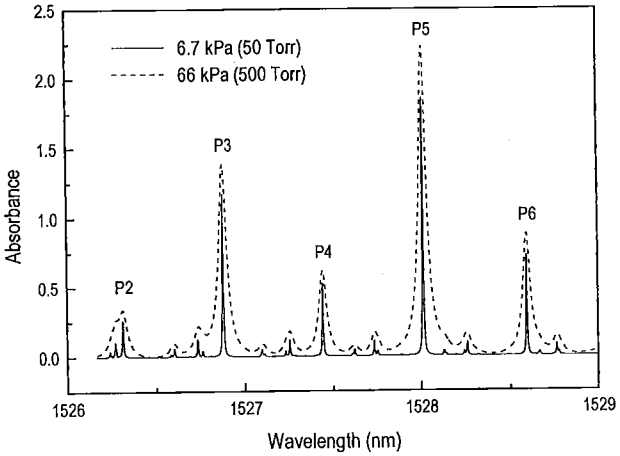


Fig. 4. Plot of $^{12}C_2H_2$ absorbance $\alpha L$ between 1526 and 1529 nm for the low- and the high-pressure cells.

The apparent shift due to smaller lines is most significant for the broader high-pressure lines, where small lines can be buried within the primary line. We estimated the effect of these lines by modeling the worst cases. The high-pressure data were modeled with Lorentzian line shapes that approximate the spectra in the vicinity of lines $R1$, $P4$, and $P14$. These primary lines had small lines located ~35 pm from their line centers. The line parameters were obtained from the low-pressure data, with the linewidths scaled up to account for pressure broadening. White noise was added to the pure Lorentzian shapes to simulate real data. We initially limited the line fitting to the central portion of the line within 85% of the maximum absorbance. Adding small lines, modeled as described above, resulted in a shift in the line center value returned by the fitting program for the (modeled) primary line. We found that the fitted line center of the primary line is most sensitive to additional lines that are very near the line center. Even a very small line (absorbance ≈1% of the primary line) can cause an apparent line shift of ~0.2 pm if it is within 50 pm of the center of the primary line. In our modeling of the three primary lines the apparent shift due to small neighboring lines was as much as 0.4 pm, and the reduced $\chi^2$ value was as large as 6. Restricting the fit range to the central portion of the line, within 65% of the maximum absorbance, reduced the $\chi^2$ values to ~1, indicating a good fit, and restored the original (unperturbed) line center. Restricting the fit range further did not significantly effect the results.

We compared the modeling results with those obtained from the measured data and observed similar trends. For the high-pressure data, primary lines with nearby weak lines gave relatively poor fits ($\chi^2$ between 1.6 and 3.4) when fitted over 85% of the maximum absorbance. Narrowing the fit range to within 65% of maximum absorbance reduced the $\chi^2$ values to ~1 and changed the fit-

ted line center by as much as 0.2 pm; further narrowing of the fit range had a negligible effect.

The combination of avoiding primary lines with significant nearby lines and reducing the fit range to within 65% of the maximum absorbance eliminates the line-overlap skewing effect for most cases. To first order, the small line wings could be approximated by a slope in the background when the fit was restricted to a narrow region around the line center. The fitting program was able to remove this effect by removing a slope in the region of the main line. If the fit range was too wide, however, the simple slope approximation was not adequate. Since we cannot be certain that there are no small lines closer than 35 pm from a primary line center, we assign a standard uncertainty (estimated standard deviation) for each of the relative line centers: of 0.07 pm for the high-pressure data and 0.04 pm for the intermediate-pressure data, owing to residual effects of additional lines. These uncertainty estimates are derived from the variation of the line centers as we changed the width of the fitting region. In view of the good $\chi^2$ values obtained, we believe that this uncertainty estimate is conservative.

### C. Line Fitting Reproducibility

To test the reproducibility of the line fit we took several scans of the same lines and determined the pressure shift for each scan. Since the wavelength meter could drift slightly between each scan, we compared only the shift measurement, not the individual line center measurements. From these measurements we estimate that the standard deviation for the line shift is 0.03 pm. Since this is an uncertainty in the shift measurement and not an uncertainty in the individual line centers, we then divide this value by $\sqrt{2}$ and assign a standard uncertainty of 0.02 pm for both the low-pressure and the higher-pressure cell data.

**Table 1. Uncertainty Budget**[a]

| Source of Uncertainty | Relative Line Center Standard Uncertainty (pm) | | |
|---|---|---|---|
| | Low-Pressure Cell (6.7 kPa) | Intermediate-Pressure Cell (29.7 kPa) | High-Pressure Cell (66 kPa) |
| Nearby line contribution | – | 0.04 | 0.07 |
| Fit statistical uncertainty | 0.02 | 0.02 | 0.02 |
| Fit reproducibility | 0.02 | 0.02 | 0.02 |
| Combined standard uncertainty | $u_c$(low) = 0.03 | $u_c$(int) = 0.05 | $u_c$(high) = 0.08 |

[a] This uncertainty budget was used for the determination of relative line centers for the low-, intermediate-, and high-pressure cells. The combined standard uncertainties are the root SS of the standard uncertainties due to the sources listed. The absolute accuracy of the wavelength meter is not included.

**Table 2. Pressure Shift Results**[a]

| Line | Intermediate – Low Pressure $\Delta P$ = 23.0 ± 0.6 kPa | | High – Low Pressure $\Delta P$ = 59.3 ± 1.3 kPa | | Weighted Average | |
|---|---|---|---|---|---|---|
| | Shift (pm) | Shift Slope (pm/kPa) | Shift (pm) | Shift Slope (pm/kPa) | Shift Slope (pm/kPa) | Shift Slope (MHz/Torr) |
| *R*27 | 0.99(12) | 0.043(5) | 2.56(17) | 0.043(3) | 0.043(2) | −0.73(3) |
| *R*17 | 0.72 | 0.031 | 1.89 | 0.032 | 0.032(2) | −0.55(3) |
| *R*11 | 0.53 | 0.023 | 1.39 | 0.023 | 0.023(2) | −0.39(3) |
| *R*7 | 0.39 | 0.017 | 1.02 | 0.017 | 0.017(2) | −0.29(3) |
| *R*1 | 0.15 | 0.007 | 0.46 | 0.008 | 0.008(2) | −0.14(3) |
| *P*3 | 0.37 | 0.016 | 0.98 | 0.017 | 0.016(2) | −0.27(3) |
| *P*4 | 0.42 | 0.018 | 1.02 | 0.017 | 0.017(2) | −0.29(3) |
| *P*5 | 0.40 | 0.017 | 1.01 | 0.017 | 0.017(2) | −0.29(3) |
| *P*6 | – | – | 0.96 | 0.016 | 0.016(3) | −0.27(5) |
| *P*10 | 0.35 | 0.015 | 1.02 | 0.017 | 0.017(2) | −0.29(3) |
| *P*13 | 0.35 | 0.015 | 0.98 | 0.017 | 0.016(2) | −0.27(3) |
| *P*14 | 0.37 | 0.016 | 0.98 | 0.017 | 0.016(2) | −0.27(3) |
| *P*23 | 0.50 | 0.022 | 1.36 | 0.023 | 0.023(2) | −0.39(3) |
| *P*24 | – | – | 1.44 | 0.024 | 0.024(3) | −0.41(5) |
| *P*25 | 0.58 | 0.025 | 1.53 | 0.026 | 0.026(2) | −0.44(3) |

[a] Pressure shift results obtained from the two cell pairs for the measured lines of the $\nu_1 + \nu_3$ band of acetylene $^{12}C_2H_2$ are shown. The uncertainties in the final digits of the values are indicated in parentheses. For the data in columns 2–5, all the values in a particular column have the uncertainty listed for the first value in the column. The uncertainties quoted are the expanded uncertainties obtained by use of a coverage factor $k = 2$ (i.e., our quoted uncertainty is $\pm 2\sigma$).

### D. Wavelength Accuracy

Although the absolute accuracy of the wavelength measurement was not relevant to the pressure shift measurement, extrapolating our line center measurements to zero pressure and comparing with literature values serves as a good verification of our measurements. To determine the line center accuracy for our measurements we first checked the accuracy of the wavelength meter used in the measurements. We have set up a high-accuracy wavelength reference for this purpose.[2] Diode laser light at 1560.5 nm is amplified with an erbium-doped fiber amplifier and is frequency doubled in a periodically poled lithium niobate crystal. The resultant 780-nm light is then used to conduct saturated absorption spectroscopy on the $5S_{1/2} \rightarrow 5P_{3/2}$ transitions of rubidium ($^{85}$Rb and $^{87}$Rb). The line centers of the hyperfine components of these transitions have been measured with an uncertainty of ±0.4 MHz (Ref. 9); a subset of these lines has been measured to higher accuracy.[10] We stabilized the laser to several different hyperfine components of the $^{87}$Rb transition and compared the wavelength meter reading (vacuum wavelength) to the literature values multiplied by 2. Since the lines were very narrow (less than 10 MHz), the absolute stability of the laser was much better than the quoted wavelength meter uncertainty of 1 part in $10^7$ (~20 MHz at 1560 nm). From measurements taken before and after our pressure shift scans we found that the wavelength meter reading was offset by $-0.20 \pm 0.06$ pm ($+25 \pm 8$ MHz). The uncertainty ($2\sigma$) is derived from the standard deviation of 10 measurements made over a six-month period. During this time the wavelength meter offset varied from −0.16 to −0.23 pm.

## 3. PRESSURE SHIFT, LINE CENTER, AND PRESSURE BROADENING RESULTS

The uncertainty budget for the relative line center determinations is given in Table 1. Table 2 summarizes the line-shift measurement results for the low–intermediate-pressure pair and the low–high-pressure pair. We determined a weighted average slope for the pressure shift for each line. In all cases the wavelength shift was positive with increasing pressure. Figures 5(a) and 5(b) are plots of line center versus pressure for the measured lines of the $R$ and the $P$ branches, respectively. As expected, each line's shift is consistent with a linear dependence on pressure. For most of the lines in the $P$ branch, the shift was approximately +0.017 pm/kPa (or, equivalently, $+2.3 \times 10^{-3}$ pm/Torr or −0.29 MHz/Torr). The $R$ branch exhibited more variation in the pressure shift, with an approximately linear dependence on line number. For both branches, the pressure shift was considerably larger for lines far from the band center (i.e., transitions between states with high rotational quantum numbers), rising to +0.043 pm/kPa for line $R27$.

Using the line center data adjusted for the wavelength meter offset discussed in Subsection 2.D, we extrapolated the line centers to zero pressure, using linear regression fitting. Table 3 summarizes our determinations of the line centers and compares them to the more accurate measurements reported in Ref. 3, which were measured at 1–4 Pa (10–30 mTorr). Our expanded uncertainty is 0.1 pm (coverage factor of 2), which is twice the root SS of the relative line center standard uncertainty (0.03 pm), the wavelength meter calibration standard uncertainty (0.03 pm), and the linear regression fit uncertainty (0.03 pm). The estimated uncertainty given in Ref. 3 is $1.2 \times 10^{-6}$ nm. All our line center values are in good agreement with those of Ref. 3; the differences between our measurements and those reported in Ref. 3 are within our uncertainty for each line center. This gives us further confidence in our analysis of the line center values.

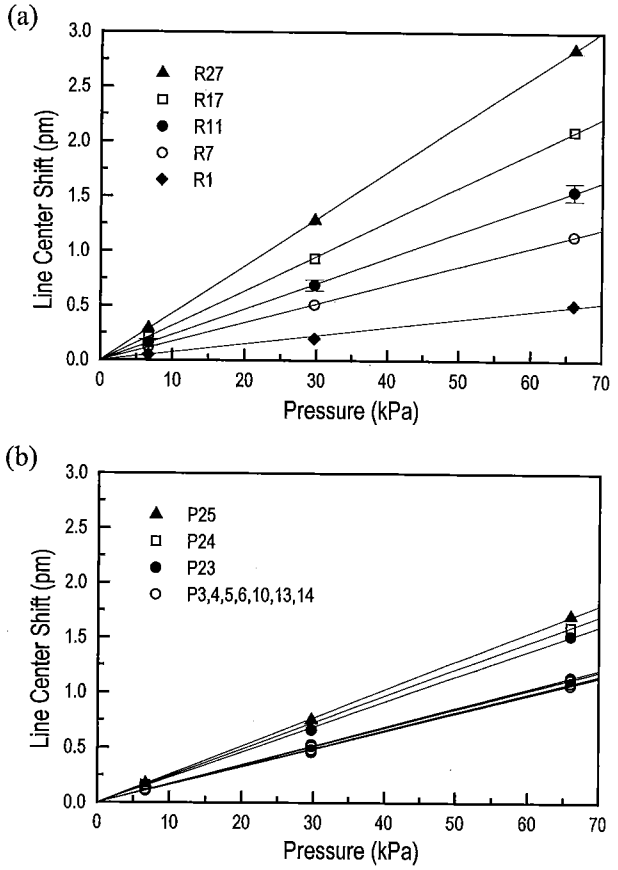


Fig. 5. (a) Pressure shift of the line centers for the measured lines in the $^{12}C_2H_2$ $R$ branch. Each line is shown with a linear least-squares fit to the data. (b) Pressure shift of the line centers for the measured lines in the $^{12}C_2H_2$ $P$ branch, with corresponding linear least-squares fits. The uncertainties for the other data shown in (a) and (b) are the same as those shown for $R11$.

Pressure broadening is responsible for the Lorentzian component of the Voigt line shape. We found that the pressure broadening also varied with line number. In contrast to the pressure shift dependence, however, the pressure broadening was largest for lines near the band center (transitions between states with low rotational quantum numbers). Table 4 summarizes our results for the width of the Lorentzian component of the Voigt line shape, where the Gaussian component (which is due to Doppler broadening at room temperature) was fixed at 3.7 pm. The width variation with line number can be seen more clearly in Fig. 6, where we plot the Lorentzian component of the linewidth for the lines measured in the $R$ branch and the associated linear fit results. The Lorent-

zian linewidth slope versus pressure, derived from these least-squares fits, is also given in Table 4. Our uncertainty for the Lorentzian linewidth values was derived from the variation that we observed when using different fitting algorithms for the Voigt profile. Although the fitting algorithms agreed for the line centers, values for the Lorentzian component of the linewidth differed slightly.

**Table 3. Unperturbed Line Center Values[a]**

| Line | Line Center This Measurement (nm) | Line Center from Ref. 3 (nm) | Difference (pm) |
|---|---|---|---|
| *R*27 | 1512.45242 | 1512.45244 | −0.02 |
| *R*17 | 1516.44113 | 1516.44109 | 0.04 |
| *R*11 | 1519.13678 | 1519.13671 | 0.07 |
| *R*7 | 1521.06034 | 1521.06029 | 0.05 |
| *R*1 | 1524.13602 | 1524.13604 | −0.02 |
| *P*3 | 1526.87430 | 1526.87424 | 0.06 |
| *P*4 | 1527.44111 | 1527.44103 | 0.08 |
| *P*5 | 1528.01428 | 1528.01421 | 0.07 |
| *P*6 | 1528.59388 | 1528.59379 | 0.09 |
| *P*10 | 1530.97621 | 1530.97616 | 0.05 |
| *P*13 | 1532.83042 | 1532.83034 | 0.08 |
| *P*14 | 1533.46131 | 1533.46125 | 0.06 |
| *P*23 | 1539.42979 | 1539.42977 | 0.02 |
| *P*24 | 1540.12535 | 1540.12528 | 0.07 |
| *P*25 | 1540.82729 | 1540.82727 | 0.02 |

[a] Line center results for very-low-pressure conditions (less than 5 Pa). Our measurements (column 2) are values obtained by use of line centers at the different pressures extrapolated to zero pressure. Our expanded uncertainty for each line center is $1 \times 10^{-4}$ nm (0.1 pm). The data in column 3 are from Ref. 3, measured at very low pressure with an estimated uncertainty of $1.2 \times 10^{-6}$ nm.

**Table 4. Pressure Broadening Results[a]**

| | Lorentzian Component of Linewidth (pm) | | | Linewidth Slope | |
|---|---|---|---|---|---|
| Line | 6.7-kPa Cell | 29.7-kPa Cell | 66-kPa Cell | (pm/kPa) | (MHz/Torr) |
| *R*27 | 3.3(8) | 13.3(8) | 29.4(8) | 0.44(2) | 7.5(3) |
| *R*17 | 4.3 | 18.3 | 40.2 | 0.61 | 10.1 |
| *R*11 | 4.9 | 22.6 | 50.2 | 0.76 | 13.0 |
| *R*7 | 5.1 | 23.5 | 51.6 | 0.78 | 13.3 |
| *R*1 | 6.1 | 25.2 | 55.8 | 0.84 | 14.3 |
| *P*3 | 5.9 | 24.7 | 54.2 | 0.81 | 13.8 |
| *P*4 | 5.6 | 23.5 | 51.9 | 0.78 | 13.3 |
| *P*5 | 5.4 | 22.7 | 50.5 | 0.76 | 13.0 |
| *P*6 | 5.3 | – | 48.1 | 0.72 | 12.3 |
| *P*10 | 5.0 | 20.6 | 45.3 | 0.68 | 11.6 |
| *P*13 | 4.9 | 20.6 | 44.9 | 0.67 | 11.4 |
| *P*14 | 4.7 | 19.7 | 43.1 | 0.65 | 11.1 |
| *P*23 | 3.9 | 15.7 | 34.4 | 0.51 | 8.7 |
| *P*24 | 3.7 | – | 33.4 | 0.50 | 8.5 |
| *P*25 | 3.6 | 15.6 | 32.3 | 0.48 | 8.2 |

[a] Width of the Lorentzian component of the Voigt line profile derived from fitting the lines with the Gaussian component, which is due is Doppler broadening, fixed at 3.7 pm. Results were obtained at the three pressures for selected lines of the $\nu_1 + \nu_3$ band of acetylene $^{12}C_2H_2$. All the values in a column have the expanded uncertainty (coverage factor of 2) listed for the first value in the column.

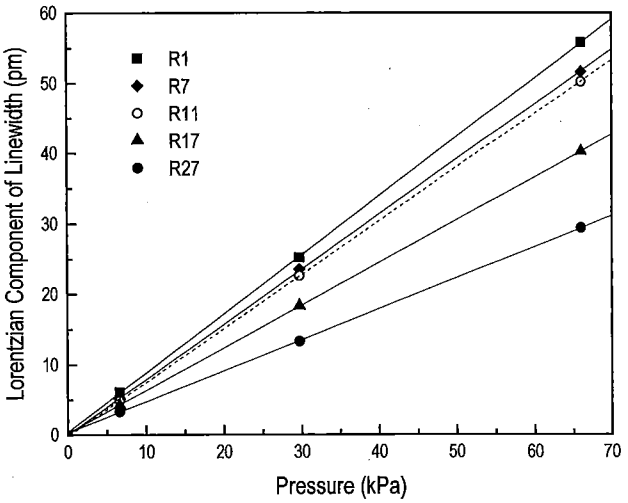


Fig. 6. Pressure broadening (Lorentzian component of the linewidth) for the measured lines in the $^{12}C_2H_2$ *R* branch. Each line is shown with a linear least-squares fit to the data. The uncertainties are approximately the same size as the data points.

We attribute this result to the fact that the Voigt profile is generated numerically; small differences between algorithms can yield different model parameters. Since each line is a convolution of its Gaussian and Lorentzian components, the convolved linewidth at low pressure will be dominated by the width of the Gaussian component.

Our pressure broadening analysis does not include the small effect of collisional narrowing due to velocity averaging. This effect is negligible at higher pressures, where pressure broadening dominates, but can cause the line shape to deviate from the expected Voigt profile at low pressures.[11] Since we do not observe significant discrepancies between our data and the Voigt function, we conclude that the line-shape modification due to collisional narrowing is negligible at the level of our quoted uncertainty.

## 4. SPECTRAL SENSITIVITY TO OTHER ENVIRONMENTAL CONDITIONS

Other environmental conditions can affect molecular spectra and can potentially shift line centers. For normal conditions, all these effects are small compared with the pressure shift and broadening described in Section 3. Below we discuss the effects of temperature variation and electromagnetic fields.

### A. Temperature

Aside from the obvious effect that thermal distribution of population in rotational levels has on line strengths, thermally induced changes in molecular spectra are usually small for moderate temperatures. Moderate thermal changes can slightly modify the pressure shift and broadening of a molecular line by changing the collision frequency; both these collision-induced effects are proportional to the density of collision partners and their mean relative velocity.[4] In a closed cell containing only the gas phase, the density is fixed. The mean relative velocity is

proportional to the square root of the temperature. Thus the temperature dependence of the pressure shift, $\Delta\nu(T)$, is simply

$$\Delta\nu(T) = \Delta\nu(T_m)\sqrt{T/T_m}, \quad (2)$$

where $\Delta\nu(T_m)$ is the pressure shift measured at temperature $T_m$ and the temperatures $T$ and $T_m$ are in degrees Kelvin. From Eq. (2) it can be seen that the line center is fairly insensitive to temperature changes; a 50 K increase from room temperature would increase the pressure shift by only 8%. For the measurements reported here, the temperature was (22 ± 2) °C. This temperature range would cause a ±0.3% change in the pressure shift, which is negligible compared with our other sources of uncertainty.

### B. Electromagnetic Fields

An excellent discussion of the effects of electromagnetic fields on molecular spectra can be found in Ref. 12. The ground state of acetylene and most other molecules is the $^1\Sigma$ electronic state, where the angular momentum of the electronic cloud is zero. Consequently, magnetic field effects such as hyperfine structure (arising from the internal magnetic field) and the Zeeman effect (interaction of a magnetic moment with an external magnetic field) are much smaller than those normally found in atoms. This is simply due to the nature of the molecular chemical bond, where unpaired electrons in atoms pair up with electrons from another atom. Magnetic moments for these molecules are proportional to the overall rotational angular momentum and are ~1/1000 that of an electron. Thus a moderately large magnetic field of 0.1 T (1000 G) would cause a Zeeman splitting of less than 1 MHz (~0.01 pm).

Electric quadrupole hyperfine structure (arising from the interaction of a nuclear electric quadrupole moment and the surrounding charge distribution) is absent in acetylene because it lacks a nuclear quadrupole moment. First- and second-order Stark shifts (arising from the interaction of the molecular electric dipole moment and an external electric field) are also absent; owing to its symmetry, the molecule has no permanent electric dipole moment. An electric field can polarize a molecule; this effect is $\sim 10^4$ times smaller than second-order Stark effects and is therefore negligible, except in the case of extremely high electric fields.[12]

High-intensity ac electric fields can split and shift line centers.[12] This effect is referred to as the Autler–Townes effect, the ac Start effect, or light shift and is significant when the laser intensity is comparable with the saturation intensity $I_S$ of a transition. The saturation intensity has been estimated for line $P13$ of $^{13}C_2H_2$ (Ref. 13) as $I_S\,(\mathrm{W/m^2}) = 15 \times 10^6(0.1 + 10p)^2$ where $p$ is the pressure in torr. For the lowest pressure used in our work (6.7 kPa = 50 Torr), this gives a saturation intensity of $4 \times 10^8\ \mathrm{W/cm^2}$. Our measurements were made with an intensity of less than $1\ \mathrm{W/cm^2}$, so we are clearly operating far from the regime in which this effect is significant. This effect may need to be taken into account for experiments done at low pressure and high intensity, such as those in which a power buildup cavity is used.

## 5. CONCLUSIONS

We have measured the pressure-induced shift for 15 lines of the $\nu_1 + \nu_3$ rotational–vibrational band of acetylene $^{12}C_2H_2$. Although there is some variation with line number, over half the lines measured exhibit a shift near +0.017 pm/kPa (or, equivalently, $+2.3 \times 10^{-3}$ pm/Torr or −0.29 MHz/Torr). We have also measured the pressure broadening of these lines and find that it also varies with line number and is typically ~0.7 pm/kPa (12 MHz/Torr). For a pressure of 27 kPa (~200 Torr, the conditions of NIST Standard Reference Material 2517[1]), the line shift is typically near 0.5 pm but can be as large as 1.2 pm for lines far from the band center and can be as low as 0.2 pm for lines near the band center. The Lorentzian component of the linewidths at this pressure varies from 12 pm (1.5 GHz) for lines far from the band center to 23 pm (2.9 GHz) near the band center.

Although the pressure shift and the pressure broadening are both due to the interactions of molecules during collisions, they depend on line number rather differently. The pressure shift is largest for lines far from the band center (transitions between states with high rotational quantum number $J$), whereas the pressure broadening is largest for lines near the band center (transitions between states with low $J$). One explanation for the pressure broadening line dependence is that rotational averaging of the potential during a collision causes states with high rotational angular momentum (high $J$) to be perturbed less than states with low $J$. The pressure shift is more difficult to interpret; it represents the difference between the shift of the excited state and the shift of the ground state. We would need to conduct a more extensive study before drawing any conclusions about the shift of a particular state. Measurements of the pressure broadening and the pressure shift of carbon monoxide lines[14] show trends that are very similar to those that we observe in acetylene.

We also evaluated the line sensitivity to temperature changes and to electromagnetic fields. We conclude that these effects are small compared with the collision-induced pressure broadening and pressure shift. In most cases thermal and electromagnetic effects can be neglected, although they can be significant at extreme temperatures and field strengths.

## ACKNOWLEDGMENTS

The authors are grateful to C. Wang for discussions and suggestions on the uncertainty analysis and to D. Nesbitt and L. Hollberg for discussions and comments on the manuscript.

S. Gilbert can be reached by e-mail at sgilbert@boulder.nist.gov.

## REFERENCES

1. S. L. Gilbert, T. J. Drapela, and D. L. Franzen, "Moderate-accuracy wavelength standards for optical communications," in *Technical Digest—Symposium on Optical Fiber Measurements*, NIST Spec. Publ. 839 (National Institute of Standards and Technology, Boulder, Colo., 1992), pp. 191–194; S. L. Gilbert and W. C. Swann, "Acetylene $^{12}C_2H_2$ ab-

sorption reference for 1510–1540 nm wavelength calibration—SRM 2517," NIST Spec. Publ. 260–133 (National Institute of Standards and Technology, Gaithersburg, Md., 1998).
2. S. L. Gilbert, W. C. Swann, and C. M. Wang, "Hydrogen cyanide $H^{13}C^{14}N$ absorption reference for 1530–1560 nm wavelength calibration—SRM 2519," NIST Spec. Publ. 260–137 (National Institute of Standards and Technology, Gaithersburg, Md., 1998).
3. K. Nakagawa, M. de Labachelerie, Y. Awaji, and M. Kourogi, "Accurate optical frequency atlas of the 1.5-$\mu$m bands of acetylene," J. Opt. Soc. Am. B **13**, 2708–2714 (1996).
4. W. Demtröder, *Laser Spectroscopy*, 2nd ed. (Springer-Verlag, Berlin, 1996), pp. 67–82.
5. Y. Sakai, S. Sudo, and T. Ikegami, "Frequency stabilization of laser diodes using 1.51–1.55 $\mu$m absorption lines of $^{12}C_2H_2$ and $^{13}C_2H_2$," IEEE J. Quantum Electron. **28**, 75–81 (1992).
6. B. N. Taylor and C. E. Kuyatt, "Guidelines for evaluating and expressing the uncertainty of NIST measurement results," NIST Tech. Note 1297 (National Institute of Standards and Technology, Gaithersburg, Md., 1993).
7. P. A. Boggs, R. H. Byrd, J. E. Rogers, and R. B. Schnabel, "User's reference guide for ODRPACK version 2.01: software for weighted orthogonal distance regression," NIST Interagency Rep. 4834 (National Institute of Standards and Technology, Gaithersburg, Md., 1992).
8. A. Baldacci, S. Ghersetti, and K. N. Rao, "Interpretation of the acetylene spectrum at 1.5 $\mu$m," J. Mol. Spectrosc. **68**, 183–194 (1977); G. Guelachvili and K. N. Rao, *Handbook of Infrared Standards II* (Academic, San Diego, Calif., 1993), pp. 564–571.
9. G. P. Barwood, P. Gill, and W. R. C. Rowley, "Frequency measurements on optically narrowed Rb-stabilised laser diodes at 780 nm and 795 nm," Appl. Phys. B: Photophys. Laser Chem. **53**, 142–147 (1991).
10. J. Ye, S. Swartz, P. Jungner, and J. L. Hall, "Hyperfine structure and absolute frequency of the $^{87}Rb\,5P_{3/2}$ state," Opt. Lett. **21**, 1280–1282 (1996).
11. P. L. Varghese and R. K. Hanson, "Collisional narrowing effects on spectral line shapes measured at high resolution," Appl. Opt. **23**, 2376–2385 (1984).
12. C. H. Townes and A. L. Schawlow, *Microwave Spectroscopy* (Dover, New York, 1975), Chaps. 10 and 11.
13. M. de Labachelerie, K. Nakagawa, and M. Ohtsu, "Ultranarrow $^{13}C_2H_2$ saturated-absorption lines at 1.5 $\mu$m," Opt. Lett. **19**, 840–842 (1994).
14. J. Henningsen, H. Simonsen, T. Møgelberg, and E. Trudsø, "The $0 \rightarrow 3$ overtone band of CO: precise linestrengths and broadening parameters," J. Mol. Spectrosc. **193**, 354–362 (1999).